

# Size induced arrest of the room temperature crystallographic structure in nanoparticles of $\text{La}_{0.5}\text{Ca}_{0.5}\text{MnO}_3$

Tapati Sarkar,<sup>1,a)</sup> A. K. Raychaudhuri,<sup>1</sup> and Tapan Chatterji<sup>2</sup>

<sup>1</sup>*DST Unit for NanoSciences, Department of Material Science, S.N. Bose National Centre for Basic Sciences, Block JD, Sector III, Salt Lake, Kolkata 700 098, India*

<sup>2</sup>*Science Division, Institut Laue-Langevin, BP 156, 38042 Grenoble Cedex 9, France*

We have shown, using high resolution x-ray diffraction studies of nanoparticles, that size reduction can lead to an arrest of the high temperature phase in perovskite materials, which prevents growth of the low temperature phase that needs a specific crystal structure for its stabilization. This has been shown in the context of  $\sim 15$  nm diameter nanocrystals of  $\text{La}_{0.5}\text{Ca}_{0.5}\text{MnO}_3$ , in which the orthorhombic distortion at room temperature freezes in and, as a consequence, the charge order cannot set in and the ferromagnetic state that sets in at higher temperature is stabilized at low temperature.

Engineering the physical properties of bulk solids by reducing their size to a few nanometers is an area of intense topical interest. The possibility that new properties arise when the size can be tuned to a suitable range allows one to synthesize materials with different properties by keeping the chemistry the same. The size tuning of physical properties is expected to be most effective in materials that have competing interactions. In this context, the perovskite oxides present a particularly interesting class of materials. In such oxides, the ground state is often determined by a specific crystallographic structure. In this letter, we explore the possibility whether the crystallographic structure can be arrested by size reduction so that it does not evolve when the temperature is varied and the ground state specific to the bulk does not stabilize at low temperature. Instead, the high temperature phase is stabilized. Our investigation has been carried out on the hole doped perovskite oxide manganites (with  $\text{ABO}_3$  structure), which have interactions of different types that are often of comparable strengths.<sup>1</sup> This makes them quite fascinating because the ground state can have distinct phases [a ferromagnetic metal, a charge ordered (CO) insulator, or a paramagnetic polaronic insulator] which are energetically close.<sup>2</sup> The different phases stabilize as ground state at different ranges of the hole concentration. When we reduce the particle size of these manganites to the order of 15–20 nm (henceforth referred to as nanomanganites), various finite size effects come into play, making the study of these systems even more interesting. It has been recently shown that in such nanomanganites, when the size is reduced below 100 nm, the charge and orbitally ordered (CO-OO) ground state with antiferromagnetic spin order becomes unstable and this gives rise to a ferromagnetic ground state.<sup>3,4</sup> This has been achieved by size reduction without altering the hole concentration (or the stoichiometry). However, the cause of such destabilization is still an open issue in the absence of a systematic investigation on the effect of size reduction on the structure of such systems. In this context, a precision temperature dependent structural investigation is important because the stability of the CO-OO phase depends on the structure. This letter addresses this specific issue and shows that

in such nanomanganites (with size down to  $\sim 15$  nm), the room temperature structure gets arrested and does not develop on cooling. Finite size effect does not allow supercell modulation (needed for such ordering) to develop and has been suggested as one of the mechanisms that can prevent growth of the CO-OO phase.

We have chosen for our study the half-doped manganite  $\text{La}_{0.5}\text{Ca}_{0.5}\text{MnO}_3$  (LCMO), which has a paramagnetic-ferromagnetic phase transition at around 225 K ( $T_C$ ) followed by the charge ordering transition at  $T_{\text{CO}}=155$  K.<sup>5</sup> An antiferromagnetic spin order accompanies the CO-OO phase, which is stabilized by distinct structural transition,<sup>5</sup> as will be discussed below. The nanoparticles were prepared by a polyol precursor based route.<sup>6,7</sup> For comparison to the standard data, we prepared a bulk sample (particle size  $\sim 3$   $\mu\text{m}$ ) by sintering the same particles at higher temperatures. The high resolution powder diffraction data were obtained at the European Synchrotron Radiation Facility, Grenoble, France by using the BM-01B beamline and a wavelength of 0.375 Å, over the temperature range of 5–300 K. Nearly 5000–6000 points/scan using six detectors were taken. To our knowledge, this is the first study of the structural evolution of nanoparticles of manganites by using high resolution diffraction techniques. The magnetic measurements have been carried out by using a Quantum Design superconducting quantum interference device magnetometer<sup>8</sup> and also a homemade low field ac susceptibility bridge working at 33.33 Hz. Microstructural characterization was done by using field emission gun scanning electron microscopy (SEM) and transmission electron microscopy (TEM). The TEM data show that the nanoparticles are good single crystals with a size of  $\sim 15 \pm 3$  nm. This matches well with the size determined from the x-ray data obtained by using a Williamson–Hall plot.<sup>9</sup> The size of the larger “bulk” particles (diameter  $\sim 3$   $\mu\text{m}$ ) were determined by SEM. In Fig. 1, we show the temperature evolution of the lattice parameters for the bulk as well as for the nanoparticle samples. The lattice parameters have been obtained by using the Rietveld powder diffraction profile fitting technique. We have used the orthorhombic space group  $Pnma$  by following Radaelli *et al.*<sup>5</sup> The lattice parameters of bulk LCMO display large changes in the region  $T_{\text{CO}} < T < T_C$ . At 300 K, the three axes have simi-

<sup>a)</sup>Electronic mail: tapatis@bose.res.in

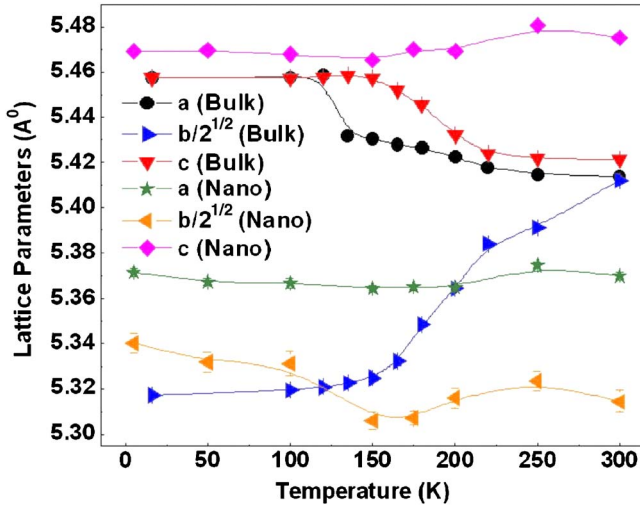


FIG. 1. (Color online) Variation of lattice parameters for bulk and nano-LCMO. Error bars, where not visible, are smaller than the symbols.

lar size. On cooling, the  $b$  axis drastically decreases and the  $a$  and  $c$  axes correspondingly increase. The changes become more pronounced below 200 K, and they become nearly temperature independent for  $T < T_{CO}$ . However, for the nanoparticle sample, the lattice parameters virtually remain unchanged throughout the temperature range studied. The small changes in the lattice parameters of the nanoparticles on cooling do not follow any systematic trend, unlike that in the bulk sample. In the nanoparticle, the  $a$  axis at room temperature is smaller by  $\approx 1\%$ , the  $b$  axis is smaller by  $\approx 2\%$ , while the  $c$  axis expands by  $\approx 1\%$ .

The cell volume and the orthorhombic strains ( $O_{S_{\perp}}$  and  $O_{S_{\parallel}}$ ) in the two samples are shown in Fig. 2. The cell volume decreases by about 1.6% in the nanoparticle sample. The orthorhombic strain  $O_{S_{\parallel}}$  gives the strain in the  $ac$  plane and is defined as  $O_{S_{\parallel}} = 2(c-a)/(c+a)$ , while  $O_{S_{\perp}}$  gives the strain along the  $b$  axis with respect to the  $ac$  plane and is defined as  $O_{S_{\perp}} = 2(a+c-b\sqrt{2})/(a+c+b\sqrt{2})$ . In the bulk sample, the largest change occurs in  $O_{S_{\perp}}$ , which increases as the sample

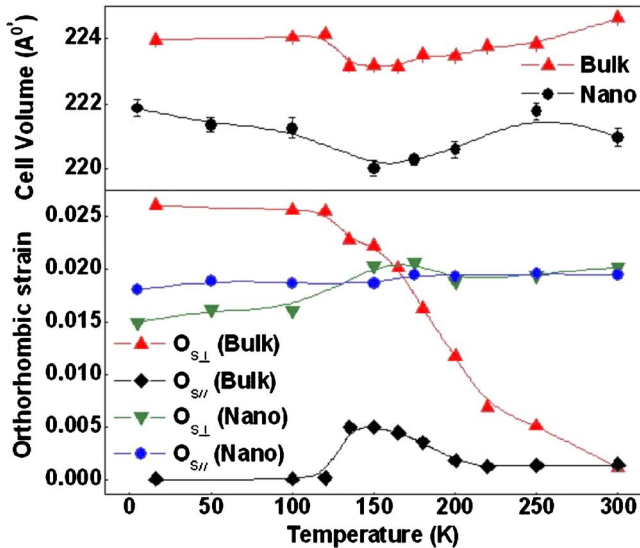


FIG. 2. (Color online) Variation of the cell volume and orthorhombic strains for bulk and nano-LCMO. Error bars, where not visible, are smaller than the symbols.

is cooled and reaches a saturating value of 0.026 below the charge ordering temperature  $T_{CO}$ . On the other hand,  $O_{S_{\parallel}}$  shows a modest value over the whole temperature range. It shows a small enhancement in the temperature range  $T_{CO} < T < T_C$  and decreases to nearly 0 for  $T < T_{CO}$ . On the other hand, in the nanoparticle sample, the orthorhombic strains are isotropic ( $O_{S_{\perp}} \approx O_{S_{\parallel}}$ ), and they remain more or less temperature independent. No clear changes can be detected near any of the transitions. The room temperature structure is thus arrested in the nanocrystals.

From the temperature evolution of the various structural parameters, it is quite clear that although the high temperature structure of the nanoparticles has greater orthorhombic strains than that of the bulk sample, since the room temperature structure is arrested, this distortion gets frozen and does not increase any further on cooling. The low temperature structure that supports the long range CO-OO in the bulk sample cannot evolve in the nanocrystals. The low temperature CO phase is monoclinic,<sup>5</sup> which happens due to a large  $O_{S_{\perp}}$  and a very small  $O_{S_{\parallel}}$ . The near equality of  $O_{S_{\perp}}$  and  $O_{S_{\parallel}}$  in the nanoparticle sample prevents formation of the proper structure. The development of CO phase needs creation of a modulated structure and a supercell, as has been seen in bulk samples of LCMO.<sup>5</sup> The propagation vector of the CO modulated structure is  $(1/2 + \epsilon, 0, 0)$ , where  $\epsilon \approx 0.01$ . This implies that the periodicity of the supercell is  $\approx 200a \approx 106$  nm. Thus, if the particle size is less than  $\sim 100$  nm, the supercell modulation needed for the CO phase cannot develop. In our case, the size of the nanocrystals is more than seven times less than this value.

One of the reasons which cause the structure to freeze might be an increased surface pressure acting on the nanoparticle sample. Assuming the particles to be spherical in shape, there is a surface pressure  $P = 2S/d$ , where  $d$  is the diameter of the particle and  $S$  is the surface tension. The exact value of  $S$  for manganites is not known, but for perovskite oxide titanates,  $S \approx 50$  N/m.<sup>10</sup> For larger particle size ( $> 100$  nm), the pressure is not substantial and is of not much consequence. However, for a particle size of  $\approx 15$  nm, we get an estimated  $P \approx 6$  GPa. This surface pressure in manganites can be substantial and can have the same effect as hydrostatic pressure. This hypothesis is strongly supported when we compare our data for the nanoparticle sample to that recently reported by Kozlenko *et al.*,<sup>11</sup> in which they have studied the evolution of the structure of bulk LCMO under hydrostatic pressures. Our data for the nanoparticle sample (which we consider to be under an effective pressure of  $\sim 6$  GPa) matches very well with their data for bulk sample under the same pressure. Thus, high surface pressure combined with any strain effects present in the nanoparticle sample might occur in tandem to arrest the structure of the nanoparticle sample so that it cannot form the CO phase on cooling. We note that in manganites, the bulk modulus is rather large ( $\approx 190$  GPa). As a result, even a 2% volume change of the unit cell will need an energy of  $\approx 0.08$  eV, which is larger than the thermal energy, which, as a result, cannot destabilize the arrest of the room temperature structure in the nanocrystals.

The size induced arrest of the structure in nano-LCMO is reflected in its physical properties, which shows that the CO transition is destabilized and the ferromagnetic state is stable at low temperature. As an example, in Fig. 3, we show

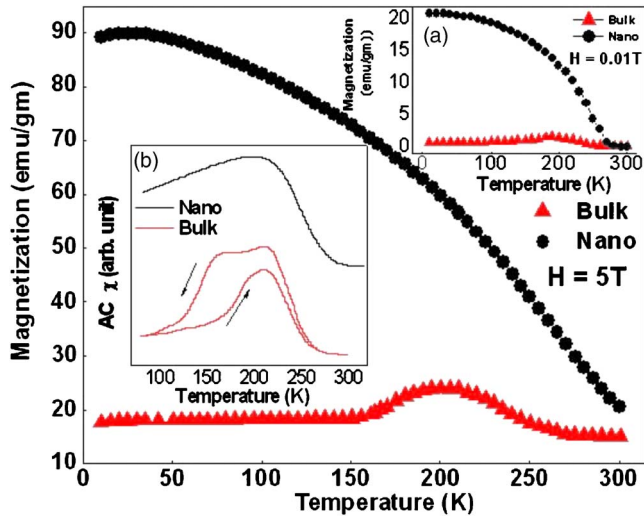


FIG. 3. (Color online) Field cooled magnetization vs temperature for bulk and nano-LCMO under magnetizing fields of 0.01 T [inset (a)] and 5 T. Inset (b) shows the ac susceptibility data for the two samples.

the field cooled magnetization versus temperature data for both samples under two magnetizing fields, 0.01 T [inset (a) of Fig. 3] and 5 T. Inset (b) of Fig. 3 shows the ac susceptibility data. The bulk sample, as expected, shows the ferromagnetic transition and a sudden drop in the magnetization at  $\sim 155$  K, indicating the presence of the antiferromagnetic transition which accompanies the charge ordering transition. The hysteresis in the ac susceptibility seen in the bulk sample near  $T_{CO}$  is a signature of the transition. In the nanoparticle sample, we see no such signature of any antiferromagnetic transition. In contrast, in the nanocrystals, the ferromagnetic behavior that sets in at  $T_c \approx 255$  K remains stable until the lowest measured temperature of 10 K with a total ferromagnetic moment of  $\approx 3.18 \mu_B/\text{f.u.}$ , which is 91% of the expected moment when we have full ferromagnetic alignment of spins. This sample also shows a clear hysteresis

loop in the  $M$ - $H$  curve with a coercive field of  $\approx 400$  Oe at  $T=5$  K, which is the same as seen in ferromagnetic compositions, such as LCMO.

To conclude, we have shown that size reduction can lead to an arrest of the high temperature phase in perovskite materials, such as manganites, which will prevent the structures to evolve on cooling and, thus, destabilize the ground state (at low temperatures), such as the CO state that depends on specific crystallographic structures.

The authors thank Dr. Hermann Emerich of the E.S.R.F, Grenoble, France for help during data acquisition. We also thank Dr. P. Chowdhury of CGCRI, Kolkata, India for his help in the Rietveld refinements of the data. We thank the Department of Science and Technology of the government of India for financial support. One of the authors (T.S.) thanks the UGC of the government of India for the fellowship.

- <sup>1</sup>J. B. Goodenough, *Phys. Rev.* **100**, 564 (1955).
- <sup>2</sup>*Colossal Magnetoresistance, Charge Ordering and Related Properties of Manganese Oxides*, edited by C. N. R. Rao and B. Raveau (World Scientific, Singapore, 1998).
- <sup>3</sup>S. S. Rao, K. N. Anuradha, S. Sarangi, and S. V. Bhat, *Appl. Phys. Lett.* **87**, 182503 (2005).
- <sup>4</sup>C. L. Lu, S. Dong, K. F. Wang, F. Gao, P. L. Li, L. Y. Lv, and J. M. Liu, *Appl. Phys. Lett.* **91**, 032502 (2007).
- <sup>5</sup>P. G. Radaelli, D. E. Cox, M. Marezio, and S. W. Cheong, *Phys. Rev. B* **55**, 3015 (1997).
- <sup>6</sup>T. Sarkar, B. Ghosh, and A. K. Raychaudhuri, *J. Nanosci. Nanotechnol.* **7**, 2020 (2007).
- <sup>7</sup>T. Sarkar, P. K. Mukhopadhyay, A. K. Raychaudhuri, and S. Banerjee, *J. Appl. Phys.* **101**, 124307 (2007).
- <sup>8</sup>MPMS SQUID magnetometer, 6325 Lusk Boulevard, San Diego, CA 92121-3733, USA.
- <sup>9</sup>G. K. Williamson and W. H. Hall, *Acta Metall.* **1**, 22 (1953).
- <sup>10</sup>Z. H. Zhou, X. S. Gao, J. Wang, K. Fujihara, S. Ramakrishna, and V. Nagarajan, *Appl. Phys. Lett.* **90**, 052902 (2007).
- <sup>11</sup>D. P. Kozlenko, L. S. Dubrovinsky, I. N. Goncharenko, B. N. Savenko, V. I. Voronin, E. A. Kiselev, and N. V. Proskurnina, *Phys. Rev. B* **75**, 104408 (2007).